Vol. 636: 221–234, 2020
https://doi.org/10.3354/meps13222

MARINE ECOLOGY PROGRESS SERIES
Mar Ecol Prog Ser

Published February 20

Integrated mixed-effect growth models for species with incomplete ageing histories: a case study for the loggerhead sea turtle *Caretta caretta*

Brandon E. Chasco[1,2,*], James T. Thorson[2,3], Selina S. Heppell[2], Larisa Avens[4], Joanne Braun McNeill[4], Alan B. Bolten[5], Karen A. Bjorndal[5], Eric J. Ward[6]

[1]Fish Ecology Division, National Marine Fisheries Service, NOAA, Newport, OR 97365, USA
[2]Department of Fisheries and Wildlife, Oregon State University, Corvallis, OR 97331, USA
[3]Habitat and Ecological Processes Research Program, Alaska Fisheries Science Center, NMFS, NOAA, Seattle, WA 98115, USA
[4]Protected Resources Branch, Southeast Fisheries Science Center, National Marine Fisheries Service, NOAA, Beaufort, NC 28516, USA
[5]Archie Carr Center for Sea Turtle Research and Department of Biology, University of Florida, Gainesville, FL 32611, USA
[6]Conservation Biology Division, Northwest Fisheries Science Center, NOAA, Seattle, WA 98115, USA

ABSTRACT: For stochastic growth processes, integrated mixed-effects (IME) models of capture–recapture data and size-at-age data from calcified structures such as otoliths can reduce bias in model parameters. Researchers have not fully explored the performance of IME models for simultaneously estimating the unknown ages, growth model parameters, and derived variables. We simulated capture–recapture observations for tagging experiments and skeletochronology (i.e. humerus growth) observations for stranded loggerhead sea turtles *Caretta caretta* based on previously published parameter estimates for 3 growth processes (logistic, Gompertz, and von Bertalanffy). We then fit IME models to the integrated and non-integrated data. For the integrated data (both tagging and skeletochronology), we found decreased bias and uncertainty in estimated growth parameters and ages, and decreased misspecification of the growth process based on AIC. Applying the IME model to Western Atlantic loggerheads, the von Bertalanffy growth process provided the best fit to the skeletochronology data for the humeri from 389 stranded turtles and capture–recapture data from 480 tagged turtles. The estimated mean growth coefficient (μ_k) and mean asymptotic straight carapace length (μ_∞) were equal to 0.076 yr^{-1} and 92.1 cm, respectively. The estimated mean ages of the stranded turtles and recaptured tagged turtles were 13.5 and 14.6 yr, respectively. Assuming the size-at-sexual maturity (SSM) is 95% of the asymptotic size, the mean and 95% predictive interval for the age-at-sexual maturity (ASM) was 38 (29, 49) yr. Our results demonstrate that IME models provide reduced bias of the growth parameters, unknown ages, and derived variables such as ASM.

KEY WORDS: Somatic growth · Integrated mixed-effect models · Skeletochronology · Capture–recapture · Age-at-sexual maturity

1. INTRODUCTION

Somatic growth models play an essential role in species management. Among aquatic taxa, growth models are critical for determining vital rates such as natural mortality and age-at-sexual maturity (Charnov 1993, Jensen 1997, Prince et al. 2015, Then et al. 2015, Thorson et al. 2017), and mapping length-frequency data to age or staged structured population models (Fournier & Archibald 1982, Caswell 1989, Fournier et al. 1998). In spite of their importance, estimating the parameters in growth models

*Corresponding author: brandon.chasco@noaa.gov

can be exceedingly difficult (Schnute 1981). The parameters in popular growth models (e.g. logistic, von Bertalanffy, and Gompertz) are highly correlated, and the temporal and spatial heterogeneity in aquatic habitats and resources can mask the differences between the measurement error in the data and the variability in the growth process (Aires-da-Silva et al. 2015, D'Arcy & Thorson 2015).

To reduce the bias for parameters that are difficult to estimate, and to appropriately account for the different sources of uncertainty (i.e. observation error versus process error) for highly stochastic processes, researchers have focused on a class of models referred to as integrated mixed-effects (IME) models (Royle & Dorazio 2008, Kéry & Schaub 2012). The 'mixed-effect' part of an IME model uses random effects to describe sources of process uncertainty such as within-individual variability over time (i.e. transient variability) and or between-individual variation within a population (e.g. persistent variability) (de Valpine 2002, Thorson & Minto 2015). The 'integrated' part of an IME forces the parameters of the model to reconcile all of the available data simultaneously (Maunder & Punt 2013). IME models have been used across a range of taxa and ecological questions, such as stock assessment of marine fishes (Methot & Wetzel 2013), mark–recapture survival and movement analysis (Letcher et al. 2015), density dependence (Foss-Grant et al. 2016), and species distribution models (Thorson et al. 2017, Green et al. 2018). Similarly, the use of IME models for describing somatic growth has increased in recent years (Cope & Punt 2007, Dortel et al. 2013, Aires-da-Silva et al. 2015, D'Arcy & Thorson 2015, Maunder et al. 2016, Cadigan & Campana 2017).

For many populations, such as sea turtles (Superfamily Chelonioidea) and cartilaginous fishes (class Chondrichthyes), the resorption of the oldest interiormost growth rings on the calcified structures makes it very difficult to determine the total age (Zug et al. 1986, Taylor et al. 2005). Thus, the relationship between length and age for anything but the youngest individuals is unknown. For many of these populations, data from tagging studies provide additional growth rate information, but not size-at-age information. While some researchers have estimated unknown ages and growth parameters simultaneously with mixed-effects models (Olsen 2002, Taylor et al. 2005, Eaton & Link 2011), determining how an IME model may improve estimates of both the unknown ages and the parameters of the growth models by integrating multiple data sets (e.g. capture–recapture, tagging, biogeochemical) has not been explored.

Loggerhead sea turtles *Caretta caretta* are a protected species (Federal Register 1978, Casale & Tucker 2017) with a complex life history that includes both pelagic and neritic habitats (Mansfield et al. 2009). A goal of sea turtle demographers has been to estimate age-specific responses to specific environmental or anthropogenic perturbations (e.g. age at sexual maturity, age at stranding on beaches, and age at recruitment to fisheries by-catch; NRC 2010, Gallaway et al. 2016). However, the lack of known ages and highly variable growth rates has confounded the ability of researchers to estimate somatic growth. Furthermore, the lack of size-at-age models has limited the ability to link size-specific observations with age in integrated demographic models (Zug et al. 1986, Snover et al. 2007, Braun-McNeill et al. 2008, Avens et al. 2017, Ramirez et al. 2017).

Researchers have made considerable progress with sea turtle growth models, with models that compare growth rate data from tagged turtles and calcified bones from stranded turtles (Goshe et al. 2016), account for within- and between-individual stochastic growth rates (Bjorndal et al. 2013, Avens et al. 2017), and include exogenous estimates of missing growth rings (Zug et al. 1986, Snover et al. 2007, Petitet et al. 2012, Avens et al. 2015). However, to our knowledge, no attempts have been made to combine each of these steps in a single statistical framework and evaluate whether growth parameters and unknown ages are unbiased when estimated simultaneously. The objective of this research was to build an IME model for loggerhead sea turtle growth and compare it with previously published age–length relationships. Specifically, our IME model examines: (1) the effects of persistent (between individuals) and transient (within an individual) variability in the growth process, (2) the ability to estimate unknown ages for tagged and stranded individuals, (3) the integration of humerus growth rates of stranded turtles with carapace growth rates of recaptured tagged turtles, and (4) the bias and uncertainty for derived variables, such as age-at-sexual maturity (ASM).

2. MATERIALS AND METHODS

2.1. Data for the case study involving Western Atlantic loggerheads

Data for our IME model included previously collected humeri diameter measurements from stranded loggerhead turtles (Avens et al. 2015) and carapace growth from capture–recapture tagging studies

(Braun-McNeill et al. 2008). Between 1995 and 2011, humerus bones were collected from 389 loggerhead turtles along beaches of the Western Atlantic and 9 from the Azores in the central Atlantic (see Fig. 1 in Avens et al. 2015 and Table S1 in Avens et al. 2013). From each turtle, researchers collected the diameter of each line of arrested growth (LAG), the maximum humerus diameter, straight carapace length (SCL), and the date and location of recovery. Individual humeri were cross-sectioned and prepared following the methods of Avens et al. (2013), with LAG diameters being recorded in millimeters to the nearest 13th decimal place. The period between successive LAG measurements is equal to 1 yr; however, in 43 out of 3867 diameter measurements, the LAG markings along the measured axis were too diffuse or damaged to read accurately. Because these LAG markings were missing, the time to the next measurable LAG diameter ($\delta_{i,j,j-1}$) was inferred from the number of observable LAGs along a separate axis of the humerus. Individual turtles possessed between 2 and 33 LAGs, and the SCLs of the stranded turtles ranged from 17.6 to 108.2 cm.

Within Core and Pamlico Sounds, North Carolina, USA, between 1992 and 2012 (Braun-McNeill et al. 2008), 480 loggerhead sea turtles were captured and recaptured. Loggerheads were tagged with Inconel tags at the trailing edge of each rear flipper and injected with a subcutaneous passive integrated transponder (PIT) tag. Standard (notch-to-tip) SCL measurements were collected to the nearest millimeter. SCL at tagging ranged from 25 to 106 cm and the number of recaptures ranged between 1 and 12, with an average of 1.7. The average time-at-liberty ranged from 1 d to 15.5 yr, with an average of 381 d. Short recapture intervals are essential, as they likely reflect measurement error, not variability in the growth process. Most (95%) of the turtle recaptures occurred between May and November, with November being the peak month for both tagging and recapture (31% of total captures).

2.2. IME model of carapace growth

Our IME modeling framework combined data from skeletochronology and tagging data for Western Atlantic loggerhead sea turtles. We created a GitHub repository (https://github.com/bchasco/IME_growth_model), which contains all of the R scripts to compile the Temple Model Builder (TMB) code (see Section 2.6), run simulation models, and reproduce the plots and figures in the results. Table 1 provides a list of parameters, variables, and data used in the model. A description of the data files (see Text S1 in the Supplement at www.int-res.com/articles/suppl/m636p221_supp.pdf), R scripts, and TMB code used to estimate and plot the results of the observed and simulated data are provided in Tables S1 & S2.

2.3. Body proportional relationship between humerus diameter and carapace size

The ratio (β) between maximum humerus diameter (max_humerus_i, mm) and the SCL_i (cm) for the i^{th} individual stranded turtle was based on the body proportional hypothesis (BPH; Francis 1990):

$$\text{max\_humerus}_i = \beta \text{SCL}_i + \epsilon_i^{\text{BPH}}, \epsilon_i^{\text{BPH}} \sim N(0, \sigma_{\text{BPH}}) \quad (1)$$

We assumed that the observation error (ϵ_i^{BPH}) was normally distributed with a standard deviation of σ_{BPH} mm.

2.4. Growth observation models

We modeled the predicted initial carapace size ($\hat{x}_{i,j=1}^d$) for both stranded and tagged turtles as:

$$x_{i,j=1}^d = f\left(L_{\infty,i}^d, k_{i,j=1}^d, L_0, a_i^d\right) \quad (2)$$

where f is a generic function (e.g. von Bertalanffy, Gompertz, or logistic; Table S3), d refers to the data stream (i.e. 'hum' for humerus from stranded turtles, or 'cr' for capture–recapture from tagged turtles), $L_{\infty,i}^d$ is the asymptotic SCL (cm) for individual i of data stream d, L_0 is the initial carapace size (cm) at age 0 and was assumed to be equal for all individuals, $k_{i,j}^d$ is the growth rate parameter with the units yr^{-1} for the first observation (j = 1) of the i^{th} individual for data stream d, and a_i^d is the estimated age in years of the first observation of the i^{th} individual for data stream d. The carapace size for each successive growth increment (Eq. 3) was modeled as a function of the growth parameters $L_{\infty,i}^d$ and $k_{i,j}^d$, the size of the humerus or carapace in the previous time-step $x_{i,j-1}^d$, and the time-at-liberty $\delta_{i,j}^d$ between observations j and $j-1$. The parameters $L_{\infty,i}^d$ and a_i^d were assumed to have persistent variation among individuals (and hence have subscript i), while growth rate $k_{i,j}^d$ was assumed to vary among individuals and observations (and therefore have subscripts i and j) to include both persistent and transient variation in growth:

$$x_{i,j>1}^d = f'\left(L_{\infty,i}^d, k_{i,j}^d, \delta_{i,j}^d; x_{i,j-1}^d\right) \quad (3)$$

The observation, or measurement, error was modeled as the difference between the model prediction

Table 1. List of subscripts, superscripts, data, and parameters of the integrated mixed-effect model for sea turtle growth

	Symbol	Description
Sub- and superscripts	i	Individual
	j	Observation
	d	Data stream: tagging (d = cr) or skeletochronology (d = hum)
Data	$O_{i,j}^{d}$	Growth observations (humerus diameter in mm, carapace length in cm) for the j^{th} observation of individual i
	SCL_i	Straight carapace length (cm) for individual i
	max_humerus_i	Maximum humerus diameter (cm) for individual i
	$\delta_{i,j}^{d}$	Time-at-liberty between j and $j-1$ for individual i
Growth process	f	Length at age model
	f'	Change in length after time-at-liberty
Fixed effects	μ_k	Average growth coefficient (yr^{-1}) of turtle
	μ_∞	Average max straight carapace length (cm)
	x_0	Carapace length at hatching (cm)
	μ_a^d	Average age of the initial observation
	β	Ratio between carapace length and humerus diameter
Random effects	$\varepsilon_{k_i}^{d}$	Persistent effects in k for data d and individual i
	$\varepsilon_{k_{i,j}}^{d}$	Transient effect in k for data d, observation j of the i^{th} individual
	$\varepsilon_{\infty_i}^{d}$	Deviations in asymptotic length for data d and the i^{th} individual
	ε_a^d	Deviations in age at first growth measurement for data d and i^{th} individual
Observation variance	$(\sigma_a^d)^2$	Variance between the observed data d and variance model predictions
	σ_{BPH}^2	Variance between paired body proportional observations
Random effects variance	ϕ_∞^2	Persistent variability in asymptotic carapace length
	$\phi_{k_i}^2$	Persistent variability in growth coefficient
	$\phi_{k_{i,j}}^2$	Transient variability in growth coefficient
	$(\phi_a^d)^2$	Variability of the age of the first observation for data type d

and the observed LAG diameters (mm) of each humerus from the stranded turtles ($O_{i,j}^{d=\text{hum}}$), or SCLs (cm) for captured and recaptured turtles ($O_{i,j}^{d=\text{cr}}$). The measurement process was different between the 2 data streams: measurements of tagged turtles were made to the nearest millimeter using calipers on wild and unsedated animals, while precision of humeri measurements were made to the nearest 1×10^{-13} mm on a computer screen with a digital image magnified at 50×. We assumed a log-normal distribution with different variances ($(\sigma^d)^2$) to describe the observation errors for the SCL measurements from capture–recaptured turtles (Eq. 4) and the LAG diameter measurements from stranded turtles (Eq. 5):

$$L\left(\log\left(\frac{O_{i,j}^{d}}{x_{i,j}^{d}}\right)\right) \sim N\left(-0.5(\sigma^d)^2, (\sigma^d)^2\right),\ d=\text{cr} \quad (4)$$

$$L\left(\log\left(\frac{O_{i,j}^{d}}{\beta x_{i,j}^{d}}\right)\right) \sim N\left(-0.5(\sigma^d)^2, (\sigma^d)^2\right),\ d=\text{hum} \quad (5)$$

2.5. Random effect for the growth process

We treated the persistent and transient variability of the growth process as random effects in the model. To distinguish between the variances for the observation and process errors, we chose σ^2 to denote the variances of the observation errors, and ϕ^2 to denote the variances of the random effects. The estimated true age of the first LAG of a humerus or first capture of a tagged turtle (a_i^d) was log-normally distributed with a mean of μ_a^d and a variance of $(\phi_a^d)^2$:

$$a_i^d = \mu_a^d \exp\left(\varepsilon_{a_i}^{d}\right),\ \ \varepsilon_{a_i}^{d} \sim N\left(-0.5\left(\phi_a^d\right)^2, \left(\phi_a^d\right)^2\right) \quad (6)$$

The correction factor for the normally distributed deviates, $-0.5(\phi_a^d)^2$, ensured that the deviates were centered at the mean and not the median.

For humeri that did possess an annulus, the LAG marking recorded during the first year of growth, the age a_i^d was assumed to be 0.75 because the time between egg deposition in the spring/summer and

the first LAG formation was less than 1 yr (Snover et al. 2007). The asymptotic SCL ($L^d_{\infty,i}$) for the i^{th} individual was normally distributed with a population mean of μ_∞ and a variance of ϕ^d_∞:

$$L^d_{\infty,i} = \mu_\infty + \varepsilon^d_{\infty_i}, \quad \varepsilon^d_{\infty_i} \sim N\left(0, \phi^2_\infty\right) \tag{7}$$

The growth coefficient for the first observation was a function of only the persistent variability between individuals ($\varepsilon^d_{k_i}$):

$$k^d_{i,j=1} = \mu_k \exp\left(\varepsilon^d_{k_i}\right) \tag{8}$$

while subsequent growth coefficients included the persistent, between-individual effect ($\varepsilon^d_{k_i}$) and transient, within individual ($\varepsilon^d_{k_{i,j}}$) effects:

$$k^d_{i,j} = \mu_k \exp\left(\varepsilon^d_{k_i} + \varepsilon^d_{k_{i,j}}\right) \tag{9}$$

The persistent and transient effects for the individuals were log-normally distributed with variances of $\varepsilon^0_{k_i}$ and $\varepsilon^0_{k_{i,j}}$, respectively:

$$\varepsilon^d_{k_i} \sim N\left(-0.5 \times \phi^2_{k_i}, \phi^2_{k_i}\right) \tag{10}$$

$$\varepsilon^d_{k_{i,j}} \sim N\left(-0.5 \times \phi^2_{k_{ij}}, \phi^2_{k_{ij}}\right) \tag{11}$$

2.6. Model fitting

The marginal likelihood of the vector of fixed effects (θ) and the variance parameters (τ) for the random effects (ϵ) given the data ($L[\text{Data}|\theta,\tau]$) was maximized by integrating across the product of the conditional probability of the data given the fixed and random effects ($\Pr(\theta,\tau|\epsilon)$), and the probability of the random effects and the estimated variances ($\Pr(\epsilon|\tau)$; Thorson & Minto 2015):

$$L[\theta,\tau|\text{Data}] = \int_\epsilon \Pr(\text{Data}|\theta,\epsilon)\Pr(\epsilon|\tau)d\epsilon \tag{12}$$

where Table 1 lists the set of fixed (μ_k, μ_∞, L_0, μ^d_a, β, σ^d, σ_{BPH}, $\phi_{\mu\infty}$, ϕ_{k_i}, $\phi_{k_{i,j}}$, ϕ^d_a) and random effects ($\varepsilon^d_{k_i}$, $\varepsilon^d_{k_{i,j}}$, $\varepsilon^d_{\infty_i}$, ε^d_a). We used the non-linear optimization package TMB (Kristensen et al. 2015) built for R (R Core Development Team 2015, version 3.6.0) to estimate the fixed and random effects of the model. TMB iteratively minimizes the joint negative log-likelihood for the fixed effects and variances of the random effects using auto-differentiation, while integrating over the likelihood of the estimates for the random effects using the Laplace approximation. To estimate the standard errors for the fixed effects, we used the inverse of the Hessian – a matrix of partial second derivatives of the likelihood with respect to each fixed effect. Random effects were predicted when setting the fixed effects at their maximum likelihood estimates, while their standard errors were estimated using the delta method while incorporating the variance of fixed effects (Kass & Steffey 1989).

Not all model combinations could be estimated due to the confounding between model parameters; in some instances, a model parameterization may contain a singularity where 2 different parameter estimates produced identical fits to the data. In these cases, the Hessian was non-positive definite, and the solution was not unique and cannot be estimated. We defined a converged model as one with a positive definite Hessian and a maximum gradient of 0.0001 for the fixed effects. To achieve the gradient threshold, we set the number of extra Newton steps taken after the outer optimization equal to 6 using the 'TMBhelper::Optimize' function in the TMBhelper package. We used the marginal Akaike's information criterion (AIC) for the fixed effects (Akaike 1974) from the 'TMBhelper package' to compare models and select the most parsimonious fit to the data.

3. RESULTS

We fit growth models to 3867 humerus diameter measurements from 398 stranded, and 1284 carapace measurements from 480 loggerhead sea turtles tagged and recaptured in the Western Atlantic between 1992 and 2012. We examined the model fits to 4 potential forms of persistent variation (both the growth coefficient and asymptotic size; the growth coefficient or the asymptotic size; and neither), 3 levels of data (integrated skeletochronology and tagging data, and individual skeletochronology or tagging data), and 3 functions approximating the growth processes (von Bertalanffy, Gompertz, and logistic). Using AIC, the von Bertalanffy growth process with persistent variability for the asymptotic size ($\varepsilon_{\infty,i}$) and transient variability for the growth coefficient ($\varepsilon^d_{k_{i,j}}$) was the best fit to the integrated data (Table 2; AIC equal to −21 054). Although not directly comparable to the integrated data using AIC, the Gompertz growth process provided the best fit for the non-integrated skeletochronology and tagging data (AIC equal to −16 243 and −5100, respectively), and was the second best fit model for the integrated data. The model with the best fit to the non-integrated skeletochronology data included persistent variance for the asymptotic size ($\varepsilon_{\infty,i}$) and growth coefficient ($\varepsilon^d_{k_i}$), and transient variability for the growth coefficient ($\varepsilon^d_{k_{i,j}}$), while the best-fit model for the non-integrated tagging data included persistent variance for only asymptotic size ($\varepsilon_{\infty,i}$). The logistic

Table 2. Parameter estimates and model diagnostics for the top 2 models (AIC: Akaike's information criterion) fit to the integrated data, the non-integrated skeletochronology, and the non-integrated tagging data. BPH: body proportional hypothesis; LAG: line of arrested growth on the humerus; PD Hessian: refers to the whether or not the model produced a positive definite Hessian; NE: parameters that were not estimated because the data to inform the parameters were not included in the model; NA: parameters that were not estimated as part of the model based on model selection (i.e. AIC) criteria. See Table 1 for definitions of the parameters

	Symbol	Integrated		Skeletochronology		Tagging	
		von Bertalanffy	Gompertz	Gompertz	von Bertalanffy	Gompertz	von Bertalanffy
Parameters	μ_∞	92.1	86.9	96	98	75.5	76.4
	μ_k	0.077	0.128	0.117	0.078	0.203	0.168
	L_0	11.9	11.7	11.7	11.7	40.5	41.2
	$\mu_a^{d=\text{hum}}$	8.6	9.9	10.8	8.5	NE	NE
	$\mu_a^{d=\text{cr}}$	13.9	15.8	NE	NE	6.9	6.6
	β	0.390	0.390	NE	NE	NE	NE
	σ_x	0.0017	0.001	0.001	0.001	NE	NE
	σ_L	0.0125	0.012	NE	NE	0.01	0.01
	σ_{BPH}	1.6498	1.6533	NE	NE	NE	NE
	$\phi_a^{d=\text{hum}}$	0.9	0.7	0.7	0.9	NE	NE
	$\phi_a^{d=\text{cr}}$	0.27	0.2	NE	NE	0.5	0.5
	ϕ_{k_i}	NA	0.23	0.3	0.4	NA	0.2
	$\phi_{k_{ij}}$	0.73	0.72	0.7	0.7	0.6	0.6
	ϕ_∞	12	11.83	12.3	10.7	8.8	8.6
Diagnostics	AIC	−21054	−20307	−16244	−16190	−5100	−5098
	PD Hessian	TRUE	TRUE	TRUE	TRUE	TRUE	TRUE
	Gradient	3.6×10^{-08}	3.4×10^{-07}	2.8×10^{-04}	2.1×10^{-05}	3.7×10^{-04}	4.4×10^{-04}

model provided a poorer fit, with ΔAICs >1000 for both the non-integrated and integrated data.

For the simulated data, visual inspection of the predicted size-at-age for the different growth processes (Gompertz, von Bertalanffy, and logistic) showed similarities for both the non-integrated and integrated skeletochronology data (Fig. 1). However, the non-integrated tagging data suggested faster growth and smaller asymptotic sizes for a given level of persistent and transient variability (Fig. 1, third column) relative to the integrated data.

A similar pattern occurred for the observed data. We found that the IME with integrated data was more similar to non-integrated skeletochronology data and less similar to non-integrated tagging data. When we compared the parameter estimates of the von Bertalanffy growth process, we found the estimated growth coefficients for the non-integrated tagging data and skeletochronology data (0.168 and 0.078 yr^{-1}, respectively) were higher than the integrated data (0.077 yr^{-1}). However, the estimated asymptotic size for the integrated data (92 cm) was between the estimates non-integrated tagging data (76 cm) and skeletochronology data (98 cm) (Table 1). For the integrated data, our estimates for the average maximum carapace growth rate were equal to 3.6 cm yr^{-1} for stranded turtles between 50 and 60 SCL (Fig. 2A), and 2.3 cm yr^{-1} for tagged turtles between 40 and 50 SCL (Fig. 2B). Both estimates are similar to other recent empirical studies (Braun-McNeill et al. 2008, Avens et al. 2013, 2015, Bjorndal et al. 2013), and show similar patterns of decreasing growth rates with increasing carapace size.

Loggerhead females reach maturity and they lay their eggs in sandy beaches: L_0 represents the theoretical size when the turtles hatch. The estimated size at age 0 (L_0) was approximately 12 cm for both integrated data and non-integrated skeletochronology data, and 41 cm for the non-integrated tagging data. Our estimate of L_0 exceeds the observed size at hatching (4.5 cm), which occurs about 2 mo after egg deposition (Miller et al. 2003).

We conducted several simulation experiments to determine how the growth processes (Gompertz, von Bertalanffy, or logistic), persistent variation ($\phi_{k_i}^d$ equal to 0.1, 0.4, 0.7), and transient variation ($\phi_{k_{i,j}}^d$ equal to 0.1, 0.4, and 0.7) affected the model selection and parameter bias. Using AIC, the simulation tests sug-

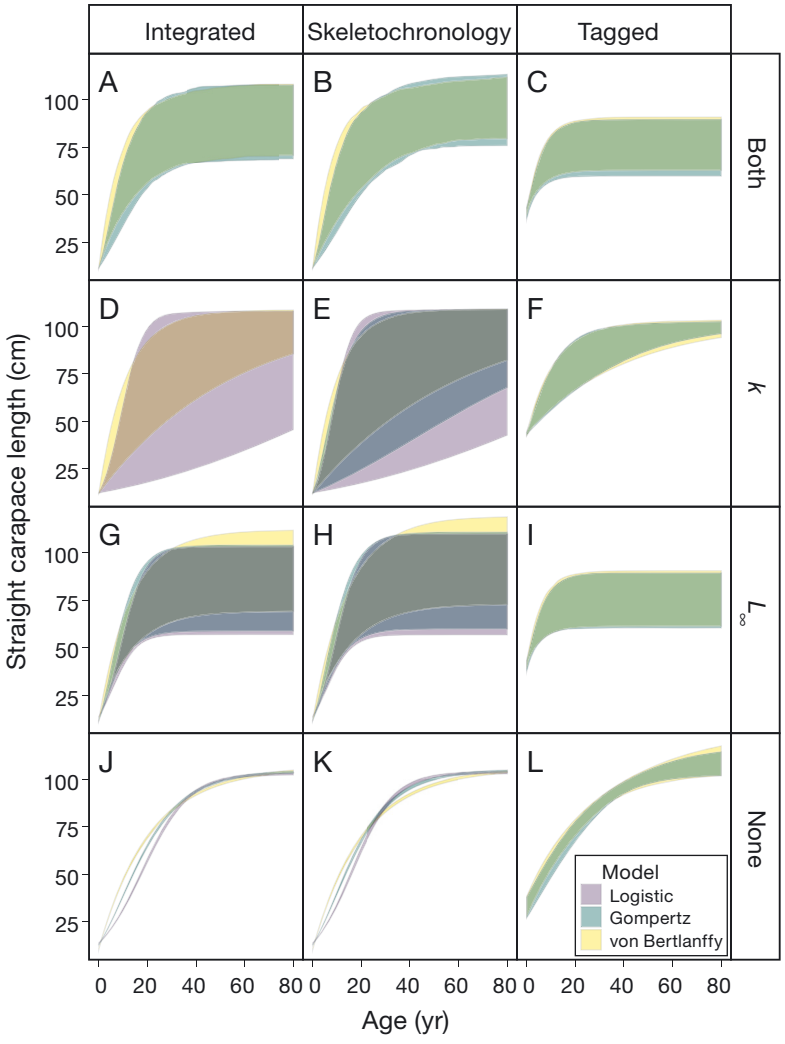

Fig. 1. A 4 × 3 × 3 factorial design examining the size (straight carapace length, SCL; cm) at age (years) for Western Atlantic loggerhead sea turtles assuming 4 levels of persistent variability (rows), 3 types of data (columns), and 3 different growth processes (color scale). Levels of persistent variability include both the growth coefficient and asymptotic size (top row); the growth coefficient (second row) or the asymptotic size (third row); or neither (bottom row). Combinations of data types include integrated data (left column), non-integrated skeletochronology data (center column), and non-integrated tagging data (right column)

gested very little misclassification of the growth process for sample sizes greater than 50 individuals (Fig. S1). Similarly, if the growth process and the level of persistent and transient variability for the model were chosen correctly, the sample size analysis indicates that the fixed effects of the model were unbiased, and the simulation error decreases with increasing sample size (Figs. S2 & S3). However, when we simulated a single growth process (e.g. von Bertalanffy) under incorrectly specified levels of persistent and transient variation for the growth coefficient, we found that AIC often misclassified the best-fit model. If the standard deviation of the persistent variation (between individuals) for the growth coefficient is <0.4 (equal to a CV of 0.42, $\sqrt{e^{\sigma^2}-1}$), and the standard deviation for the transient variation (within individuals) is >0.4, the model with only transient variation was often chosen based on AIC — a model misclassification that does not include the between-individual persistent variation (Fig. S4). Despite the misclassification of the persistent variance for the simulated data, we found little bias in the growth process parameters (Fig. S4, columns 1 and 2) except for the variation of the asymptotic size and the size at age 0 (Fig. S5R,V, respectively).

For the integrated loggerhead data from the Western Atlantic, the estimated standard deviation of the transient variability for the growth coefficient was 0.7 (CV = 0.8). Because model misclassification for the simulated data occurred for similarly high levels of transient variability, it is reasonable to assume that AIC may not have detected persistent variation in the growth coefficient that may exist. The model with the second-best fit to the integrated data includes both persistent and transient variation for the growth coefficient: this model may be a better representation of the actual growth process, despite a ΔAIC value that indicates it is not a plausible candidate model (Table 2; Burnham & Anderson 2002).

We considered the ages of the individual turtles and ASM to be essential management outcomes of the model. Based on the integrated data, the estimated mean age of the first LAG for the stranded turtles ($\mu_a^{d=\text{hum}}$) and mean age at marking for tagged turtles ($\mu_a^{d=\text{cr}}$) were 4.3 and 13.5 yr, respectively. Accounting for the total number of observed and reabsorbed LAGs, the mean age and size at stranding were 13.5 yr ($a_i^{d=\text{hum}} + \sum_j \text{LAG}_{i,j}$) and 60.2 cm SCL, respectively, and the mean age and size at last recovery for the tagged turtles were 14.8 yr ($a_i^{d=\text{cr}} + \sum_j \delta_{i,j}$)and 65.6 cm SCL (Fig. 3A,C). For the non-integrated data, the mean age at stranding increased to 16.0 yr, and the mean age at last recovery for the tagged turtles decreased to 7.5 yr (Fig. 3A,C). From our simulation experiments, we found no bias in the

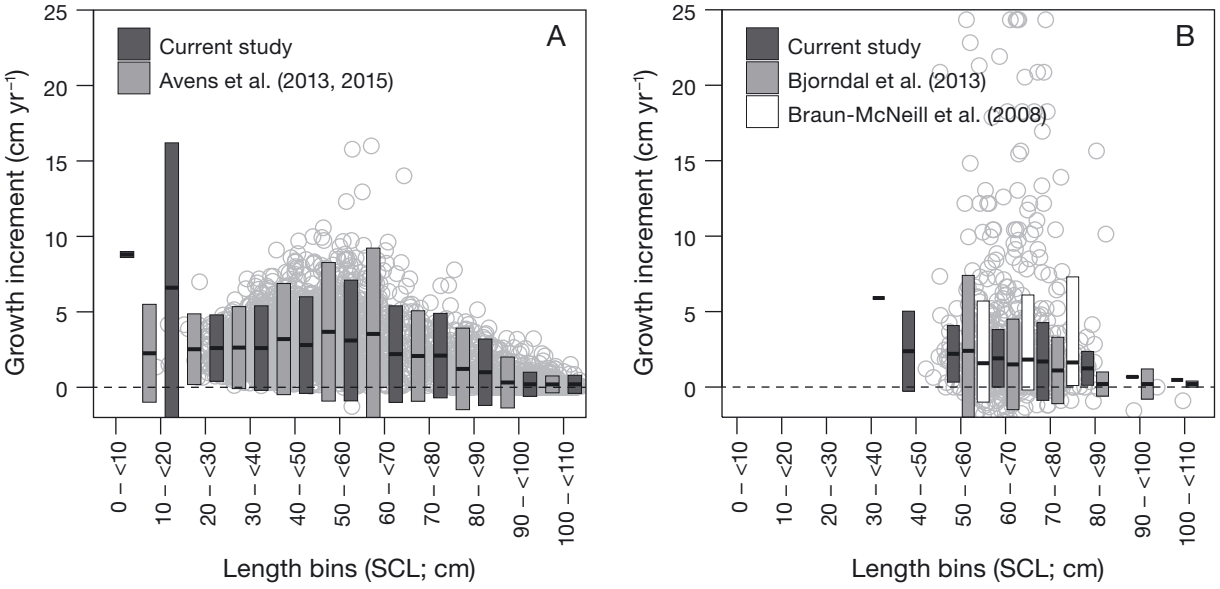

Fig. 2. Estimated carapace growth rates for (A) stranded and (B) tagged loggerhead sea turtles from the Western Atlantic between 1992 and 2012 for the current study compared to empirical estimates from Avens et al. (2015), Bjorndal et al. (2013), and Braun-McNeill et al. (2008). Horizontal lines represent the expected growth rates, and bars represent the 95% credible intervals. The grey circles are the carapace growth rates estimated from the parameters of the body proportional hypothesis (Eq. 1) and the observed humerus growth rates from line of arrested growth measurements

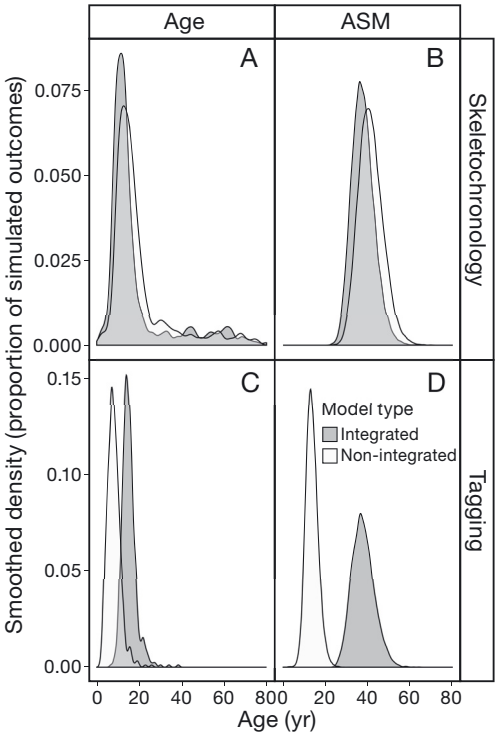

Fig. 3. A 2 × 2 × 2 factorial design of the loggerhead growth model examining 2 levels of ageing information (columns: age of individual turtles and age at sexual maturity [ASM]), 2 data types (rows: skeletochronology and tagging), and 2 levels of data integration (grey scale: non-integrated versus integrated)

initial age for either the integrated or skeletochronology data, and only a slight negative bias for the tagging data relative to the integrated data (Fig. S6). For the observed loggerhead data, the uncertainty (i.e. the standard deviation of the log-normally distributed deviates) was 0.4 for the age of the stranded turtles for both the non-integrated and integrated data, while the ageing uncertainty increased from 0.6 for the integrated data to 4.2 for non-integrated tagging data.

To quantify the uncertainty in the ASM, we simulated 100 triplets of the growth parameters (e.g. $L_{\infty,i}$, k, and L_0) for each stranded individual based on their estimated mean and covariance matrix. We found the uncertainty in the estimated ages increased with size (Fig. 4): the mean and 95% credible interval for a 40 cm SCL individual was 5 (4, 9) yr and 21 (14, 52) yr for an 80 cm SCL (Fig. 4). The estimate of $ASM_{0.95}$ was based on a random vector of growth parameters and a random draw of size at sexual maturity ($SSM_{0.95}$; refer to Text S3 in the Supplement). For the integrated data, the median and 95% probability interval for the $ASM_{0.95}$ was 38 (29, 49) yr and the $SSM_{0.95}$ was 92 (78, 106) cm (Figs. 3B,D & 4). The median and 95% probability intervals for $ASM_{0.95}$ and $SSM_{0.95}$ estimates based on the non-integrated skeletochronology data and tagging data were 31 (21, 54) and 13 (8, 20) yr, respectively, with corresponding $SSM_{0.95}$ of 99 (77, 113) and 75 (65, 89) cm.

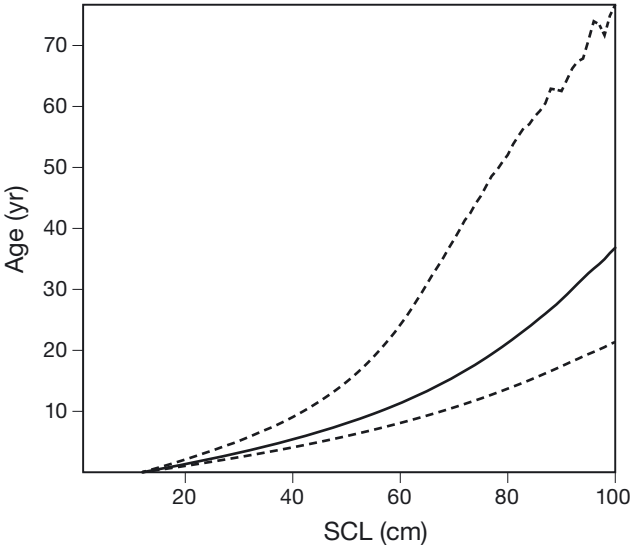

Fig. 4. Estimated age (years) for a given straight carapace length (SCL, cm) for loggerhead sea turtles in the Western Atlantic, where the dashed line is the 95% predictive interval and the solid line is the mean age (years) for an observed SCL (cm) for stranded or tagged individuals

4. DISCUSSION

Our analysis provides evidence that integrating multiple complementary data streams to address critical knowledge gaps can improve fitted models. This study demonstrates that both the skeletochronology and capture–recapture data are integral to understanding growth rates in sea turtles. Previous sea turtle research has focused on using exogenous models to estimate age rather than deriving it directly from growth increment data used to determine the parameters of the growth process (Parham & Zug 1997, Petitet et al. 2012, Avens et al. 2013). Our model treats the age of the first mark (i.e. the interior-most LAG of the stranded turtles, or the initial marking of the tagged turtles) as a parameter of the model informed directly by the growth increment data. While our simulation experiment demonstrated that the growth parameters and ageing estimates for the simulated skeletochronology and tagging data were consistent and unbiased, the parameters and ageing estimates for the observed tagging data were different for the integrated and non-integrated models (Fig. 3).

Sources of bias in the observed tagging data may include a lack of younger/smaller turtles in the sample, seasonal variability of growth (Zug et al. 1986, Chaloupka 2002, Snover & Hohn 2004), and measurement error (Braun-McNeill et al. 2008). Similarities between carapace sizes for the observed and simulated tagging data suggest that the length distribution is unlikely to bias the parameter and ageing estimates. Furthermore, the bias based on growth measurements of tagged turtles appears to be due to the recapture duration and not the seasonality of the growth. Regardless of the time of year when recaptured, individuals recaptured less than 6 mo after tagging had growth rates that were, on average, ~75% lower compared to recapture periods greater than 6 mo. Some of this bias may be due to the imprecision of the calipers used to measure tagged turtles (±0.1cm), as many of the tagged turtles with short recapture periods show zero or negative growth. Not surprisingly, the observation error for the tagged turtles is an order of magnitude higher than that of the stranded turtles, 0.0125 versus 0.0017. While previous research has excluded turtles with a time-at-liberty less than 11 mo (Bjorndal et al. 2000, Casale et al. 2009), these turtles have valuable information about the measurement error relative to the process error once seasonal growth patterns are accounted for, and they may also inform future multi-phase models exploring seasonal differences in growth. Furthermore, Fig. 5 demonstrates that these capture–recapture data are important to the integrated model because they represent a gap in carapace lengths not typically observed in skeletochronology data.

Unlike the tagged turtles, the time-at-liberty for the stranded turtles, with few exceptions, is uniformly 1 yr, the precision for the 50× magnification of humeri measurements is equal to 1×10^{-13} mm, and the specimens are dead. Furthermore, the time series of observations for stranded turtles are considerably longer, which allows more data to inform individual growth processes. In the absence of tagging data, AIC selects for both persistent and transient variability for the humerus growth processes (Table 2), which has also been demonstrated in other recent studies (Ramirez et al. 2015). However, problems with the humerus preparation persist. Depending on the orientation, cross-sections that are not perpendicular to the long axis of the humerus, or inconsistent cuts at the same point along the humerus, can result in biased measurements, although there is a close relationship between humerus diameter and SCL error associated with cross-sectioning (Snover & Hohn 2004, Snover et al. 2007).

ASM is an essential vital rate for the management of sea turtles (NRC 2010). Due to the resorption of the calcified structures, the age of the sexually mature loggerheads is challenging to observe. Thus, estimates of ASM are either derived from growth model

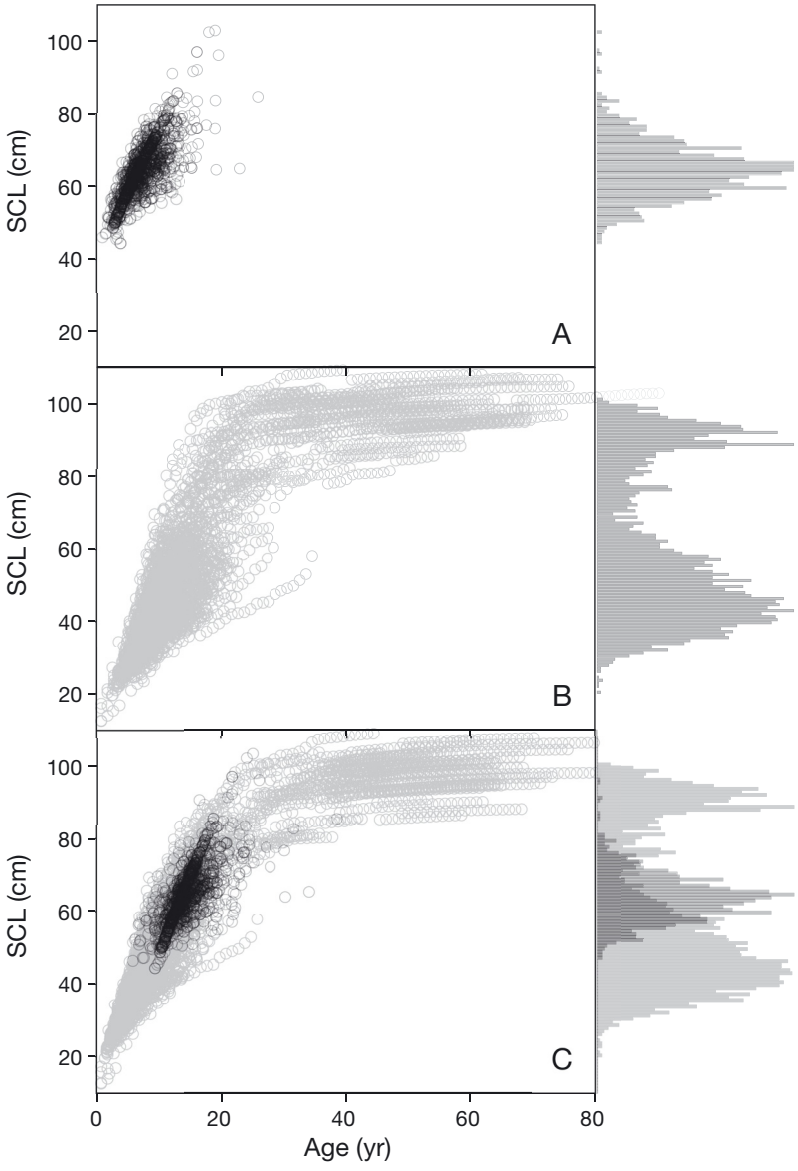

Fig. 5. Estimated size-at-age based on the (A) non-integrated tagging (dark grey circles and bars), (B) skeletochronology (light grey circles and bars), and (C) integrated data. Histograms on the right side of each plot represent the observed length frequencies of the straight carapace lengths (SCL) for each observation of the tagged loggerheads, and the estimated SCL for each line of arrested growth measurement based on the body proportional relationship

parameters or determined empirically from exhaustive tagging and recapture of hatchling turtles (Tucek et al. 2014). A recent review by Avens et al. (2015) found that ASM estimates of Western Atlantic loggerheads ranged between 24 and 42 yr for males and females. However, the variability of ASM estimates within the studies was only between 2 and 5 yr because the models assume a single fixed SSM and no individual variability in the growth process. A more reasonable assumption is that the SSM is highly variable (Avens et al. 2015, Omeyer et al. 2017), or a ratio of the asymptotic size as in our study. Using a non-parametric model of growth and SSM defined by the rapprochement, Avens et al. (2015) estimated the ASM to be 23 and 51 yr, while an analysis by Scott et al. (2012) found that the ASM of loggerhead sea turtles ranges between 38 and 52 yr with a mean of 45 yr based on transoceanic Atlantic turtles and size-at-maturity from neophyte nesters. The results from these 2 studies, which account for the growth variation using different methods, are similar to our ASM estimates based on the non-integrated skeletochronology data (21 to 54 yr), or integrated stranding and tagging data (29 and 49 yr).

Our model consistently overestimated the size at time zero (L_0). Some researchers have used non-parametric generalized additive mixed models (GAMMs) to account for the rapid growth in the first year (Avens et al. 2017, Bjorndal et al. 2017); however, GAMMs lack easily interpretable or biologically meaningful parameters, and deriving vital rates from these models is more complicated than solving for the inverse of a standard growth function (e.g. von Bertalanffy, Gompertz, logistic). The apparent bias in our initial size estimates for loggerheads is similar to other findings using multi-model frameworks to assess fish growth, where researchers found the differences in the size-at-age for a range of models are largest for age zero individuals and negligible for older individuals (Katsanevakis 2006, Smart et al. 2016). Given the importance of deriving vital rates from standard growth processes, and the minimal impact of this parameter on the estimated growth rates for older individuals, we believe the L_0 bias is acceptable.

We do not account for any size-selective bias in the skeletochronology and tagging data. Research has shown that there is size selectivity of loggerhead sea turtles by fishing gear type (Wallace et al. 2008), and that fishing mortality is partly responsi-

ble for stranded sea turtles (Crowder et al. 1995, Tomás et al. 2008, Casale et al. 2010). Research by Thorson & Simpfendorfer (2009) suggests that sufficient sample sizes and uniform sampling across collection methods are essential for estimating growth parameters. Given the low recapture probabilities of oceanic sea turtles, the logistics behind increasing the sample sizes of tagged turtles in the marine environment remains challenging. However, expanding the scope of coastal tagging studies may provide valuable insight into the latitudinal differences in loggerhead size.

In addition to the plasticity in growth associated with sea turtle life history, temporal and spatial differences in the environment may also mask the underlying growth process. Research has shown temporal and spatial growth variation at the individual (Weishampel et al. 2004, Snover et al. 2010, Ramirez et al. 2017) and population level for sea turtles (Bjorndal et al. 2013, 2017, Avens et al. 2017). Additionally, the bioenergetic costs of reproduction result in dramatic shifts in growth for both marine fishes and sea turtles (Minte-Vera et al. 2016, Avens et al. 2017). While our model does not account for any temporal and spatial deviation in growth or sex-specific differences, the integrated nature of our model provides a way of leveraging the spatial information in the tagging data with the temporal information in the skeletochronology data. We recommend that future research should conduct simulation experiments to determine whether spatial or temporal forces are detectable, given the highly variable growth processes of sea turtles.

Our current work complements the sea turtle demographic models developed over the last 4 decades (Crouse et al. 1987, Crowder et al. 1994, Heppell et al. 2005, Mazaris et al. 2005). Gallaway et al.'s (2016) recent age-structured model for Kemp's ridley sea turtles *Lepidochelys kempii* is the first attempt that we know of to fit a statistical cohort model to sea turtles using length-frequency data and a size-at-age relationship. Their estimates of the von Bertalanffy growth process, which maps cohort abundance to length-frequency data, relies entirely on capture–recapture data. While this may be appropriate for Kemp's ridley turtles, our analysis suggests that using only capture–recapture data from a single study with limited size ranges (Braun-McNeill et al. 2008) may lead to biases in the loggerhead growth process and ultimately the demographic estimates for statistical cohort analysis. The opportunity to build a statistical cohort model of Western loggerhead sea turtles exists, with over 40 yr of nester abundance from index beaches along the Western Atlantic, estimates of fishing mortality from shrimpers pre- and post-implementation of turtle excluder devices, and length-frequency data from in-water surveys (e.g. fisheries catches, capture–recapture, coastal power plant entrainments). The key to forecasting changes in cohort strength over time, however, is to understand how quickly the turtles are growing, and our model provides new insight into the importance of considering both capture–recapture and skeletochronology data when constructing that relationship.

5. CONCLUSION

Our paper presents an integrated model of sea turtle growth that estimates the ages of individuals and accounts for different sources of uncertainty from capture–recapture and skeletochronology data. Based on simulations, we have demonstrated that for the mono-phasic growth processes presented in this paper, the estimated ages and growth parameters are consistent and unbiased. The fewer number of observations per individual for the tagged turtles (i.e. an average of 1.7 recaptures per tagged individual versus to 10 LAG observations per humerus), and a narrow range of carapace lengths in our data led to biased growth parameters and ageing estimates for the non-integrated tagging data set. While our simulation experiments suggested that AIC can lead to model misclassification of the persistent variability in the growth process, this misclassification is unlikely to result in large biases of the growth parameters or the ages of individual turtles. Moving forward, we suggest that researchers consider including both skeletochronology and tagging data to estimate growth and ageing information for sea turtles. Additionally, future growth models also may be improved by considering multi-phasic models that integrate additional data streams (e.g. biogeochemical; Ramirez et al. 2015) to inform seasonal, annual, and spatial differences within and among individuals.

Acknowledgements. We thank the National Marine Fisheries Service 'Tools For Protected Species' program, which funded this research; Tomo Eguchi and Eli Holmes for the valuable input during the initial phases of this project; and the editor, 2 anonymous reviewers, and Kristin Marshall, Brian Burke, and Rich Zabel at NOAA for their internal reviews that greatly improved this manuscript. We also thank the Sea Turtle Stranding and Salvage Network. This publication was partially supported by Oregon Sea Grant under grant number NA16OAR4170190 from NOAA's

National Sea Grant College Program, U.S. Department of Commerce, and by appropriations made by the Oregon State Legislature. This publication was also supported by a grant from the Cooperative Institute for Marine Resource Studies grant, Development of quantitative tools for assessing effects of anthropogenic mortality on marine turtle populations, administered by NOAA (NB244S). The statements, findings, conclusions, and recommendations are those of the authors and do not necessarily reflect the views of these funders.

LITERATURE CITED

Aires-da-Silva AM, Maunder MN, Schaefer KM, Fuller DW (2015) Improved growth estimates from integrated analysis of direct aging and tag–recapture data: an illustration with bigeye tuna (*Thunnus obesus*) of the eastern Pacific Ocean with implications for management. Fish Res 163:119–126

Akaike H (1974) A new look at the statistical model identification. IEEE Trans Automat Control 19:716–723

Avens L, Goshe LR, Pajuelo M, Bjorndal KA and others (2013) Complementary skeletochronology and stable isotope analyses offer new insight into juvenile loggerhead sea turtle oceanic stage duration and growth dynamics. Mar Ecol Prog Ser 491:235–251

Avens L, Goshe LR, Coggins L, Snover ML, Pajuelo M, Bjorndal KA, Bolten AB (2015) Age and size at maturation- and adult-stage duration for loggerhead sea turtles in the western North Atlantic. Mar Biol 162:1749–1767

Avens L, Goshe LR, Coggins L, Shaver DJ, Higgins B, Landry AM Jr, Bailey R (2017) Variability in age and size at maturation, reproductive longevity, and long-term growth dynamics for Kemp's ridley sea turtles in the Gulf of Mexico. PLOS ONE 12:e0173999

Bjorndal KA, Bolten AB, Martins HR (2000) Somatic growth model of juvenile loggerhead sea turtles *Caretta caretta*: duration of pelagic stage. Mar Ecol Prog Ser 202:265–272

Bjorndal KA, Schroeder BA, Foley AM, Witherington BE and others (2013) Temporal, spatial, and body size effects on growth rates of loggerhead sea turtles (*Caretta caretta*) in the Northwest Atlantic. Mar Biol 160:2711–2721

Bjorndal KA, Bolten AB, Chaloupka M, Saba VS and others (2017) Ecological regime shift drives declining growth rates of sea turtles throughout the West Atlantic. Glob Change Biol 23:4556–4568

Braun-McNeill J, Epperly SP, Avens L, Snover ML, Taylor JC (2008) Growth rates of loggerhead sea turtles (*Caretta caretta*) from the western North Atlantic. Herpetol Conserv Biol 3:273–281

Burnham KP, Anderson DR (2002) Model selection and multi-model inference: a practical information-theoretic approach. Springer, New York, NY

Cadigan NG, Campana SE (2017) Hierarchical model-based estimation of population growth curves for redfish (*Sebastes mentella* and *Sebastes fasciatus*) off the Eastern coast of Canada. ICES J Mar Sci 74:687–697

Casale P, Tucker AD (2017) *Caretta caretta*. The IUCN Red List of Threatened Species. International Union for Conservation of Nature

Casale P, Mazaris AD, Freggi D, Vallini C, Argano R (2009) Growth rates and age at adult size of loggerhead sea turtles (*Caretta caretta*) in the Mediterranean Sea, estimated through capture-mark-recapture records. Sci Mar 73:589–595

Casale P, Affronte M, Insacco G, Freggi D and others (2010) Sea turtle strandings reveal high anthropogenic mortality in Italian waters. Aquat Conserv 20:611–620

Caswell H (1989) Matrix population models. Sinauer Associates, Sunderland, MA

Chaloupka M (2002) Stochastic simulation modelling of southern Great Barrier Reef green turtle population dynamics. Ecol Model 148:79–109

Charnov EL (1993) Life history invariants: some explorations of symmetry in evolutionary ecology. Oxford University Press, New York, NY

Cope JM, Punt AE (2007) Admitting ageing error when fitting growth curves: an example using the von Bertalanffy growth function with random effects. Can J Fish Aquat Sci 64:205–218

Crouse DT, Crowder LB, Caswell H (1987) A stage-based population model for loggerhead sea turtles and implications for conservation. Ecology 68:1412–1423

Crowder LB, Crouse DT, Heppell SS, Martin TH (1994) Predicting the impact of turtle excluder devices on loggerhead sea turtle populations. Ecol Appl 4:437–445

Crowder LB, Hopkins-Murphy SR, Royle JA (1995) Effects of turtle excluder devices (TEDs) on loggerhead sea turtle strandings with implications for conservation. Copeia 1995:773–779

D'Arcy NW, Thorson JT (2015) Variation in growth among individuals and over time: a case study and simulation experiment involving tagged Antarctic toothfish. Fish Res 180:67–76

de Valpine P (2002) Review of methods for fitting time-series models with process and observation error and likelihood calculations for nonlinear, non-Gaussian state-space models. Bull Mar Sci 70:455–471

Dortel E, Massiot-Granier F, Rivot E, Million J and others (2013) Accounting for age uncertainty in growth modeling, the case study of yellowfin tuna (*Thunnus albacares*) of the Indian Ocean. PLOS ONE 8:e60886

Eaton MJ, Link WA (2011) Estimating age from recapture data: integrating incremental growth measures with ancillary data to infer age-at-length. Ecol Appl 21:2487–2497

Federal Register (1978) Listing and Protecting Loggerhead Sea Turtles as 'Threatened Species' and Populations of Green and Olive Ridley Sea Turtles as Threatened Species or & 'Endangered Species'. USFWS, NMFS, NOAA, Washington, DC. http://cdn.loc.gov/service/ll/fedreg/fr043/fr043146/fr043146.pdf#page=80

Foss-Grant AP, Zipkin EF, Thorson JT, Jensen OP, Fagan WF (2016) Hierarchical analysis of taxonomic variation in intraspecific competition across fish species. Ecology 97: 1724–1734

Fournier D, Archibald CP (1982) A general theory for analyzing catch at age data. Can J Fish Aquat Sci 39: 1195–1207

Fournier DA, Hampton J, Sibert JR (1998) MULTIFAN-CL: a length-based, age-structured model for fisheries stock assessment, with application to South Pacific albacore, *Thunnus alalunga*. Can J Fish Aquat Sci 55:2105–2116

Francis RICC (1990) Back-calculation of fish length: a critical review. J Fish Biol 36:883–902

Gallaway BJ, Gazy WJ, Caillouet CW Jr, Plotkin PT and others (2016) Development of a Kemp's ridley sea turtle stock assessment model. Gulf Mex Sci 33:138–157

Goshe LR, Snover ML, Hohn AA, Balazs GH (2016) Validation of back-calculated body lengths and timing of growth mark deposition in Hawaiian green sea turtles. Ecol Evol 6:3208–3215

Green DS, Matthews SM, Swiers RC, Callas RL and others (2018) Dynamic occupancy modeling reveals a hierarchy of competition among fishers, gray foxes, and ringtails. J Anim Ecol 87:813–824

Heppell SS, Crouse DT, Crowder LB, Epperly SP and others (2005) A population model to estimate recovery time, population size and management impacts on Kemp's ridley sea turtles. Chelonian Conserv Biol 4:767–773

Jensen AL (1997) Origin of relation between K and L_{inf} and synthesis of relations among life history parameters. Can J Fish Aquat Sci 54:987–989

Kass RE, Steffey D (1989) Approximate Bayesian inference in conditionally independent hierarchical models (parametric empirical Bayes models). J Am Stat Assoc 84: 717–726

Katsanevakis S (2006) Modelling fish growth: model selection, multi-model inference and model selection uncertainty. Fish Res 81:229–235

Kéry M, Schaub M (2012) Bayesian population analysis using WinBUGS: a hierarchical perspective. Academic Press, Waltham, MA

Kristensen K, Nielsen A, Berg CW, Skaug H, Bell B (2015) TMB: automatic differentiation and Laplace approximation. J Stat Softw 70:1–21 https://arxiv.org/abs/1509.00660

Letcher BH, Schueller P, Bassar RD, Nislow KH and others (2015) Robust estimates of environmental effects on population vital rates: an integrated capture–recapture model of seasonal brook trout growth, survival and movement in a stream network. J Anim Ecol 84:337–352

Mansfield KL, Saba VS, Keinath JA, Musick JA (2009) Satellite tracking reveals a dichotomy in migration strategies among juvenile loggerhead turtles in the Northwest Atlantic. Mar Biol 156:2555–2570

Maunder MN, Punt AE (2013) A review of integrated analysis in fisheries stock assessment. Fish Res 142:61–74

Maunder MN, Crone PR, Punt AE, Valero JL, Semmens BX (2016) Growth: theory, estimation, and application in fishery stock assessment models. Fish Res 180:1–3

Mazaris AD, Fiksen Ø, Matsinos YG (2005) Using an individual-based model for assessment of sea turtle population viability. Popul Ecol 47:179–191

Methot RD Jr, Wetzel CR (2013) Stock synthesis: a biological and statistical framework for fish stock assessment and fishery management. Fish Res 142:86–99

Miller JD, Limpus CJ, Godfrey MH (2003) Nest site selection, oviposition, eggs, development, hatching, and emergence of loggerhead turtles. In: Bolten AB, Witherington BE (eds) Loggerhead sea turtles. Smithsonian Books, Washington, DC, p 125–143

Minte-Vera CV, Maunder MN, Casselman JM, Campana SE (2016) Growth functions that incorporate the cost of reproduction. Fish Res 180:31–44

NRC (National Research Council) (2010) Assessment of sea-turtle status and trends: integrating demography and abundance. National Academies Press, Washington, DC

Olsen E (2002) Errors in age estimates of North Atlantic minke whales when counting growth zones in bulla tympanica. J Cetacean Res Manag 4:185–192

Omeyer LCM, Godley BJ, Broderick AC (2017) Growth rates of adult sea turtles. Endang Species Res 34:357–371

Parham JF, Zug GR (1997) Age and growth of loggerhead sea turtles (*Caretta caretta*) of coastal Georgia: an assessment of skeletochronological age-estimates. Bull Mar Sci 61:287–304

Petitet R, Secchi ER, Avens L, Kinas PG (2012) Age and growth of loggerhead sea turtles in southern Brazil. Mar Ecol Prog Ser 456:255–268

Prince J, Hordyk A, Valencia SR, Loneragan N, Sainsbury K (2015) Revisiting the concept of Beverton–Holt life-history invariants with the aim of informing data-poor fisheries assessment. ICES J Mar Sci 72:194–203

R Core Development Team (2015) R: a language and environment for statistical computing. R Foundation for Statistical Computing, Vienna

Ramirez MD, Avens L, Seminoff JA, Goshe LR, Heppell SS (2015) Patterns of loggerhead turtle ontogenetic shifts revealed through isotopic analysis of annual skeletal growth increments. Ecosphere 6:244

Ramirez MD, Avens L, Seminoff JA, Goshe LR, Heppell SS (2017) Growth dynamics of juvenile loggerhead sea turtles undergoing an ontogenetic habitat shift. Oecologia 183:1087–1099

Royle JA, Dorazio RM (2008) Hierarchical modeling and inference in ecology: the analysis of data from populations, metapopulations and communities. Academic Press, London

Schnute J (1981) A versatile growth model with statistically stable parameters. Can J Fish Aquat Sci 38:1128–1140

Scott R, Marsh M, Hays GC (2012) Life in the really slow lane: loggerhead sea turtles mature late relative to other reptiles. Funct Ecol 26:227–235

Smart JJ, Chin A, Tobin AJ, Simpfendorfer CA (2016) Multimodel approaches in shark and ray growth studies: strengths, weaknesses and the future. Fish Fish 17: 955–971

Snover ML, Hohn AA (2004) Validation and interpretation of annual skeletal marks in loggerhead (*Caretta caretta*) and Kemp's ridley (*Lepidochelys kempii*) sea turtles. Fish Bull 102:682–692

Snover ML, Avens L, Hohn AA (2007) Back-calculating length from skeletal growth marks in loggerhead sea turtles *Caretta caretta.* Endang Species Res 3:95–104

Snover ML, Hohn AA, Crowder LB, Macko SA (2010) Combining stable isotopes and skeletal growth marks to detect habitat shifts in juvenile loggerhead sea turtles *Caretta caretta.* Endang Species Res 13:25–31

Taylor NG, Walters CJ, Martell SJ (2005) A new likelihood for simultaneously estimating von Bertalanffy growth parameters, gear selectivity, and natural and fishing mortality. Can J Fish Aquat Sci 62:215–223

Then AY, Hoenig JM, Hall NG, Hewitt DA (2015) Evaluating the predictive performance of empirical estimators of natural mortality rate using information on over 200 fish species. ICES J Mar Sci 72:82–92

Thorson JT, Minto C (2015) Mixed effects: a unifying framework for statistical modelling in fisheries biology. ICES J Mar Sci 72:1245–1256

Thorson JT, Simpfendorfer CA (2009) Gear selectivity and sample size effects on growth curve selection in shark age and growth studies. Fish Res 98:75–84

Thorson JT, Jannot J, Somers K (2017) Using spatiotemporal models of population growth and movement to monitor overlap between human impacts and fish populations. J Appl Ecol 54:577–587

Tomás J, Gozalbes P, Raga JA, Godley BJ (2008) Bycatch of loggerhead sea turtles: insights from 14 years of stranding data. Endang Species Res 5:161–169

Tucek J, Nel R, Girondot M, Hughes G (2014) Age-size relationship at reproduction of South African female loggerhead turtles *Caretta caretta.* Endang Species Res 23: 167–175

Wallace BP, Heppell SS, Lewison RL, Kelez S, Crowder LB (2008) Impacts of fisheries bycatch on loggerhead turtles worldwide inferred from reproductive value analyses. J Appl Ecol 45:1076–1085

Weishampel JF, Bagley DA, Ehrhart LM (2004) Earlier nesting by loggerhead sea turtles following sea surface warming. Glob Change Biol 10:1424–1427

Zug GR, Wynn AH, Ruckdeschel C (1986) Age determination of loggerhead sea turtles, *Caretta caretta*, by incremental growth marks in the skeleton. Smithson Contrib Zool 427:1–34

Editorial responsibility: Graeme Hays, Burwood, Victoria, Australia

Submitted: May 29, 2019; Accepted: December 16, 2019
Proofs received from author(s): February 13, 2020